Mechanism of a Photoinduced Solvent-Assisted Transfer of a Proton to a Specified Remote Target

Erik J. A. de Bekker, J. Desiree Geerlings, and Cyril A. G. O. Varma*

Leiden Institute of Chemistry, Leiden University, Gorlaeus Laboratories, P.O. Box 9502 2300 RA Leiden, The Netherlands

Received: January 5, 2000; In Final Form: March 17, 2000

Stationary and dynamic properties of the fluorescence of liquid solutions of 7-hydroxy-8-(*N*-morpholinomethyl)-quinoline (HMMQ), 2-hydroxy-1-(*N*-morpholinomethyl)-naphthalene (HMMN), and 7-hydroxyquinoline (7-HQ) have been studied as a function of temperature, solvent composition, and deuteration of the OH group in the solute. The solvents were neat *n*-hexane, neat 1,4-dioxane, neat tetrahydrofurane, or binary mixtures with a proton-accepting component. The analysis of the observations leads to a scheme for the photochemical and photophysical behavior of HMMQ in liquid solutions that differs from previous ones. It is now clear how solvents act in the catalysis of the multistep photoinduced enol−keto tautomerization of HMMQ. There are two forms of HMMQ in the ground state when the solvent contains proton acceptors (S), namely a bare form with an intramolecular H-bond and a complex in which the proton in the intramolecular H bond is also H-bonded to S. Only the latter exhibits photoinduced enol−keto tautomerization. Both forms are converted to a zwitterionic form by proton tunneling that proceeds only prior to vibrational relaxation of the excess energy deposited with the excitation. Part of the excess energy in the complex with S is used to break the intramolecular H bond and to set the protonated side group into rotational motion. The main conclusions are summarized.

Introduction

The transfer of a proton between two binding sites is frequently encountered in liquid-state chemistry and it is a process of prime importance in the functioning of biological systems.[1−3] Rate constants of proton-transfer processes span several orders of magnitude. This large span arises to a large extent from variations in the complexity of the overall transfer of the proton, which consists often of a sequence of several elementary processes. In a number of cases in which the actual transfer of the proton is rate determining, a temperature-independent kinetic deuterium isotope effect on the rate constant has been observed.[4−6] This effect provides evidence that the actual transfer of the proton is proceeding through tunneling along a H bond connecting the proton to the target. The temperature dependence of the rate constant arises then from the temperature dependence of the population of the states that allow the proton to tunnel through the potential barrier. Knowledge concerning the factors determining the potential for the proton motion is still incomplete. Interactions with the solvent may have a large effect on the rate constant, but the nature and the consequences of these interactions are not understood fully.

Single molecules of *ortho*-hydroxybenzaldehyde, 2-(2′-hydroxyphenyl)-benzothiazole, and 2-(2′-hydroxy-5′-methylphenyl)-benzotriazole dissolved in an alkane tautomerize by adiabatic excited-state intramolecular proton transfer (ESIPT) if they are in their lowest excited electronic singlet state. The tautomerization is made possible by an intramolecular hydrogen bond.[7,8] The 1:1 complexes of 2-aminopyridine (2AP) with carboxylic acids, which are held together by two H bonds, exhibit ultrafast double-proton transfer in the excited state.[9] Molecules of 7-hydroxyquinoline (7-HQ) and 2AP lack an intramolecular H bond. Nevertheless, they may exhibit ESIPT when dissolved in alkanes, but only when the solution contains H-bonded dimers of the solute or additives able to form complexes by suitable H bonding to the solute. In the enol−keto tautomerization of 7-HQ, the proton has to be transferred over the large distance of 0.6 nm separating the O and N atoms. Double-proton transfer in either a dimer with two H bonds or in a complex with two alcohol molecules is required to achieve this transfer and proton tunneling through the H bonds is rate determining.[6,10,11] The keto form of 7-HQ in an alcohol returns thermally to the enol form in a proton-transfer process with a temperature-independent kinetic isotope effect. In the examples mentioned, the nature of the H bonds is certainly important for the magnitude of the rate constant, but not in all cases is it certain that the proton tunneling is rate determining. The molecule 3-hydroxy-flavone (3HF) exhibits ESIPT when it interacts with H-bonding solvents.[8] Although the rate constant for ESIPT in 3-HF is as large as 10^{13} s^{-1}, it does not exhibit a deuterium isotope effect.[12] This result suggests that the rate constant of the actual proton transfer is much $>10^{13}$ s^{-1} and that the observed rate constant is determined by another process.

To eliminate the requirement of assistance by a complexing agent in the transfer of the proton between the donor and acceptor site in 7-hydroxyquinoline, a mobile proton acceptor has been introduced in the latter as a side group. The resulting molecule, 7-hydroxy,8-(*N*-morpholinomethyl)quinoline (HMMQ), exhibits ESIPT even when it is dissolved in non-H-bonding solvents. When it is dissolved in polar solvents and then excited by ultraviolet (UV) light, the excited enol form (E*) gets transformed into the excited keto form (K*). Overall, the transformation is simply the transfer of the proton from the OH group to the N atom (N1) in the quinoline ring. After the excitation, three steps can be clearly distinguished in this

10.1021/jp000046e CCC: $19.00
Published on Web 06/01/2000

process, namely, (step 1) adiabatic proton transfer from the OH group to the N atom (N2) in the morpholino group thereby converting E* into an excited zwitterionic form (Z*), (step 2) rotation of the protonated morpholino moiety in the side group, and (step 3) subsequent delivery of the proton at the N atom in the quinoline ring. The various stages of the process have been illustrated previously. Comparison of the stationary and time-resolved fluorescence of the compounds HMMQ, 7-hydroxyquinoline (7-HQ), and 2-hydroxy,1-(*N*-morpholinomethyl)-naphthalene (HMMN) has already provided some insight into the mechanism and dynamics of the photoinduced proton-transfer processes in HMMQ.[13−18] The difference between HMMQ and HMMN is that the quinoline ring in the former is replaced by a naphthalene ring to obtain the latter. Note that a process like the third step in the E* to K* transformation of HMMQ cannot appear in the case of HMMN. When HMMN is dissolved in polar solvents, an ESIPT process similar to step 1 in HMMQ can be observed, but unlike the case of HMMQ, the transfer of the proton from the OH group to the morpholino group does not take place when HMMN is dissolved in alkanes.[19]

The first photoinduced proton-transfer step in HMMQ just mentioned, can also be observed in the case of a solution of HMMQ in alkanes, but the subsequent steps are then inhibited.[13−16] By contrast, solutions of HMMQ in the solvent 1,4-dioxane (dielectric constant $\epsilon_D = 2.2$) exhibit excited state enol−keto tautomerization of HMMQ. Apparently 1,4-dioxane can act as a catalyst promoting the isomerization of E* into K* even in solutions of HMMQ in nonpolar solvents. Evidence has been found that the catalytic action involves a 1:1 complex in which 1,4-dioxane is H-bonded to the protonated amine of the side group.[17] In a naive picture, a large dielectric constant is thought to reduce the Coulomb attraction between the positive and negative charge in Z* sufficiently to enable rotational Brownian motion of the side group. This picture is of course not appropriate at the molecular level because there are no or just a few solvent molecules between these charges. The concept of dielectric constant does not apply then. In this respect, the important question to be answered is how the polar solvent molecules are enabling the rotational Brownian motion. Using solutions of HMMQ in properly chosen solvent mixtures, evidence has been found that the proton in the intramolecular H bond of Z* may simultaneously form a H bond with a suitable solvent molecule like 1,4-dioxane or tetrahydrofurane. As a consequence, the intramolecular H bond is then getting weaker and can be broken with less thermal excitation.[18]

The research reported in this paper is intended to provide thorough understanding of the action of solvent molecules in the complex phenomena exhibited by liquid solutions of HMMQ upon UV excitation. This report deals with the influence of temperature on the intensities of the fluorescence bands of HMMQ, with the conversion of the E* form of HMMQ into the K* form arising from its interaction with proton-accepting solvent molecules (S), and also with the effect of deuteration of the OH group in HMMQ, HMMN, and 7-HQ on their fluorescence behavior. Time-resolved spectroscopy has been applied to study the growth and decay of excited species resulting from excitation of HMMQ at fixed temperature (*T*), but when possible also as a function of *T*. Isoemissive points in the fluorescence spectrum of HMMQ have been searched for by varying *T* or the concentration of S. A general mechanism is presented, which is then adjusted to achieve agreement with the observed spectral features, with the dynamics of the primary and secondary excited species, and also with the observed effects of deuteration. The proposed mechanism differs in several respects from those suggested previously and accounts for the competition between ESIPT and vibrational relaxation of the primary excited state. The reasoning leading to the adjusted scheme is presented. New features of the complex mechanism of the simple photoinduced liquid-state proton-transfer reaction of HMMQ are now revealed.

Experimental Section

7-Hydroxy,8-(*N*-morpholinomethyl)-quinoline (HMMQ) and 2-hydroxy,1-(*N*-morpholinomethyl)naphthalene (HMMN) were prepared and purified as described previously.[1,9] *n*-Hexane, tetrahydrofurane (THF), and dichloromethane were of spectroscopic quality and were used as delivered. Sodium was added to the solvent 1,4-dioxane, which was then boiled in a refluxing apparatus for several hours until it had to be used. It was then distilled prior to use. This procedure results also in removal of oxygen from the solvent. However, some oxygen is dissolved again during sample preparation.

Absorption spectra were recorded on a Perkin-Elmer Lambda 2 UV−visible (UV−vis) spectrophotometer. Fluorescence spectra, corrected for instrumental distortions, were recorded on a Perkin-Elmer MPF-66 fluorescence spectrophotometer. Fluorescence studies were conducted using solutions of 7-HQ, HMMQ, and HMMN with concentrations of $<10^{-4}$ M. 7-HQ did not dissolve in *n*-hexane. Fluorescence spectra appearing here in the same figure have been recorded using samples with nearly equal absorbance at the wavelength selected for fluorescence excitation. The presented fluorescence intensities refer to an arbitrary fixed value of the number of absorbed photons (N_e). The small differences in the actual value of N_e have been taken into account by suitable scaling of the recorded fluorescence spectra. The resulting intensity at wavenumber λ in the fluorescence is proportional to the fluorescence quantum yield $\Phi_F(\lambda)$. The fluorescence kinetics has been studied by excitation of the sample with a 4-ps, 300-nm laser pulse and subsequent detection of the temporal development of the fluorescence with a streak camera (Hadland, Imacon 500). The time resolution achieved was 5 ps. In the case of the streak camera detection of the fluorescence of the HMMQ samples, colored glass plates were used whose optical transmission (T) is limiting the wavelength region seen by the camera. Two regions have been selected in this manner. The first one covers the region where the fluorescence from the species Z* is dominant and has been selected with a filter with maximum transmission of 55% at 393 nm that drops to 1% at 305 and 488 nm. The transmission of this filter can be described as a function of wavelength approximately as $\tau = \tau_{max} \exp[-\{(\lambda - \lambda_0)^2\}/w^2]$ with $\tau_{max} = 55\%$, $\lambda_0 = 393$ nm, and $w = 50.4$ nm. The second region is selected with a cutoff filter with $\tau = 16\%$ at 520 nm and $\tau \leq 4\%$ at 515 nm. This filter transmits only light emitted by the species K*.

The fluorescence from samples of HMMQ in *n*-hexane/5% 1,4-dioxane, *n*-hexane/5% THF, and in neat THF was studied at a number of temperatures (*T*) by inserting the sample cell in a variable-temperature optical cryostat designed to fit into the fluorescence spectrometer. The intensity of the scattered excitation light, detected as second-order diffracted light from the monochromator, was used to monitor the appearance of phase separation or crystallization on lowering the temperature. The scattered excitation light appears in the fluorescence spectra as a sharp band at 596 nm superimposed on the band arising from K*.

Deuteration of the OH group in HMMQ, HMMN, and 7-HQ was achieved by dissolving the compound in monodeuterated

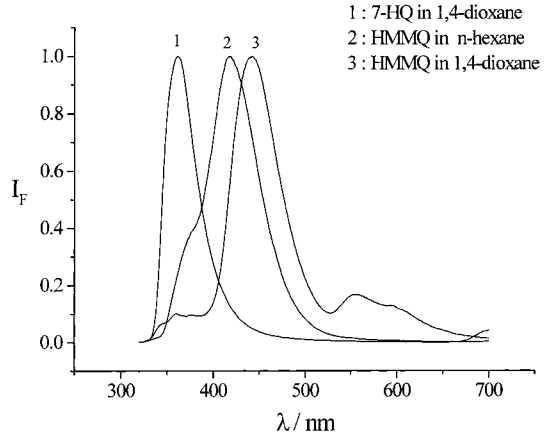

Figure 1. Fluorescence spectra of HMMQ in *n*-hexane and of HMMQ and 7-HQ in 1,4-dioxane.

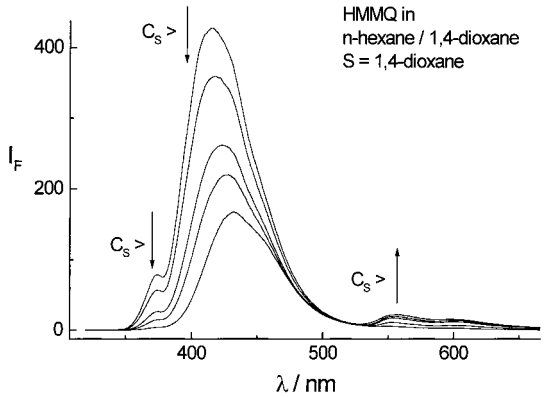

Figure 2. Changes in the fluorescence spectrum of HMMQ in *n*-hexane/1,4-dioxane arising from variation of the concentration C_S of 1,4-dioxane.

methanol (CH_3O^2H) contained in a fluorescence cell. The solvent was evaporated later on a vacuum line. The dissolving and evaporation steps were repeated twice. The dry deuterated compound in the cell was dissolved in the solvent of interest immediately after the last evaporation. Deoxygenation of the solutions was achieved by applying a number of freeze−pump−thaw cycles on the vacuum line.

Results and Discussion

Mechanism for the Conversion and Decay of Excited HMMQ. The fluorescence spectrum of HMMQ in *n*-hexane exhibits a weak band (F_E) at 370 nm and a strong band (F_Z) at 416 nm (Figure 1). A fluorescence spectrum of solutions of the compound 7-HQ in alkanes could not be obtained due to very poor solubility. The solution of 7-HQ in 1,4-dioxane shows a single fluorescence band at 361 nm. The fluorescence spectrum of the solution of HMMQ in neat 1,4-dioxane shows three bands. Two of these may be considered to arise from the same species as the bands in the spectrum of the solution of HMMQ in *n*-hexane. The band at long wavelengths (F_Z) shifts to the red and the band at short wavelengths (F_E) loses intensity in going to the solution in 1,4-dioxane. The third band (F_K) appears around 556 nm. The fluorescence spectrum of the solution of HMMQ in *n*-hexane does not show any sign of the excited form K*, but when the solution also contains some 1,4-dioxane, the fluorescence from K* can be seen clearly, as shown in Figure 2. When the concentration of 1,4-dioxane increases gradually, the band F_E disappears soon and the band F_Z shifts more and more to the red and diminishes in intensity.

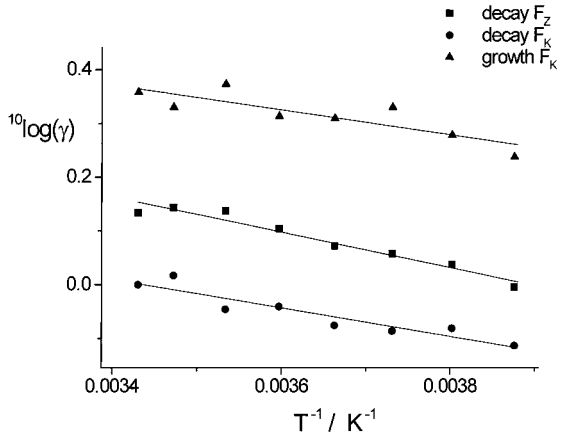

Figure 3. Temperature dependence of γ_Z, γ_{K1}, and γ_{K2} in the case of HMMQ in *n*-hexane/5% 1,4-dioxane. The quantities γ_Z, γ_{K1}, and γ_{K2} are rate constants for the decay of the band F_Z and the growth and decay of the band F_K, respectively.

After single-pulse excitation, fluorescence in the band F_Z appears instantaneously and its intensity I_Z decays monoexponentially. The time dependence of the fluorescence intensity I_K in the band F_K is biexponential and consists of a growth and a decay component. The time dependence of these intensities can be described as

$$I_Z = A_Z e^{-\gamma_Z t} \quad (1)$$

$$I_K = A_{KI} e^{-\gamma_{KI} t} + A_{K2} e^{-\gamma_{K2} t} \quad (2)$$

with $A_{K1} < 0$ and $A_{K2} = -A_{K1}$.

Figure 3 shows the observed temperature dependence of γ_Z, γ_{K1}, and γ_{K2} in the case of HMMQ in *n*-hexane/5% 1,4-dioxane. Table 1 presents the parameters in the Arrhenius description of γ_Z, γ_{K1}, and γ_{K2}. It has been reported previously that the increase of these rate constants (at ambient T) with the concentration of 1,4-dioxane is not monotonic, but reaches a plateau and then drops slowly.

Over the whole temperature range, the time constant γ_Z is substantially smaller than the time constant γ_{K1} in the growth component of F_K. This result means that the type of species emitting in the band F_Z is not the precursor of species K*. The relation $A_{K1} = -A_{K2}$ reveals that K* could be in equilibrium with its precursor. The direct precursor of K* will be referred to as Ω*. It is to be identified with the excited zwitterionic form of HMMQ in which the protonated N atom of the morpholino group (N2) has an H bond with the N atom in the quinoline ring (N1) of the excited chromophore. It is generated from an excited enol form with an intramolecular H bond by tunneling of the proton through the H bond to N2, followed by rupture of the H bond and subsequent rotation of the protonated side group to bring the proton at N2. We shall refer to this excited enol form as X*.

All the time constants plotted in Figure 3 reveal an Arrhenius-type temperature dependence, which means that each is dominated by a single rate constant. Later on we will be able to identify the dominant rate constant in each of these time constants.

The band F_Z attributed to fluorescence from a zwitterionic form appears in the fluorescence spectrum of solutions of HMMQ in alkanes. This band must arise from ESIPT to atom N2. The fluorescence spectrum of 7-HQ in 1,4-dioxane lacks the band F_Z. This result means that an excited zwitterionic form of HMMQ cannot be generated by proton transfer from excited

TABLE 1: Activation Energies of Rate Constants in the Dynamics of Photoexcited Solutions of HMMQ In *n*-Hexane/5% 1,4-Dioxane (*n*-HX/5%DX), In *n*-Hexane/5% THF (*n*-HX/5% THF), and In Neat THF (THF) Obtained from the Temperature Dependence of Experimental Rate Constants γ_Z, γ_{K1}, and γ_{K2} and Peak Intensities $I_Z(\lambda_{Zm})$ and $I_K(\lambda_{Km})$ of the Bands F_Z and F_K, Respectively, in the Range 258 < *T* < 300 K

					THF	
rate constant	*n*-HX /5% DX E_a [cm^{-1}]	intensity	*n*-HX /5% DX ϵ_Z [cm^{-1}]	*n*-HX/5% THF ϵ_Z [cm^{-1}]	ϵ_Z [cm^{-1}]	ϵ_K [cm^{-1}]
γ_Z	526 ± 9%	$I_Z(\lambda_{Zm})$	530 ± 6%	276 ± 4%	881 ± 1%	
γ_{K1}	367 ± 25%					
γ_{K2}	423 ± 15%	$I_K(\lambda_{Km})$				372 ± 4%

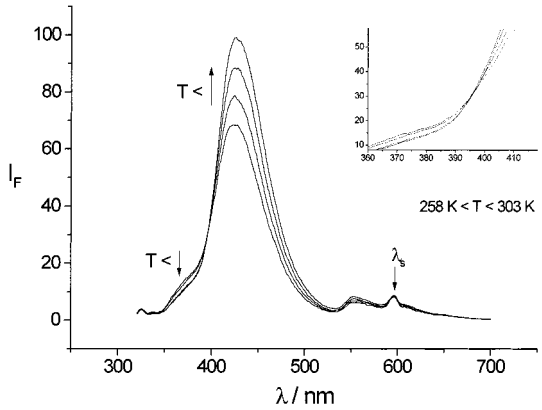

Figure 4. Changes in the fluorescence spectrum of HMMQ in *n*-hexane/5% 1,4-dioxane and light scattering at λ_s caused by temperature variations.

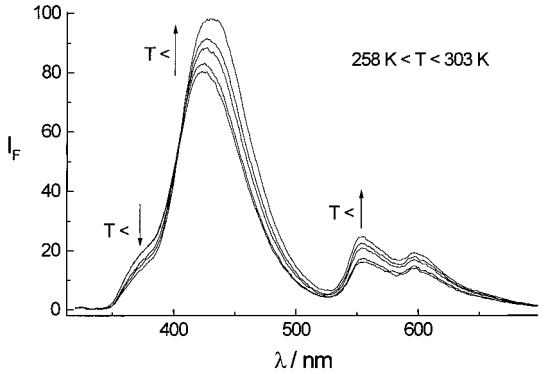

Figure 5. Changes in the fluorescence spectrrum of HMMQ in *n*-hexane/5% THF caused by temperature variations.

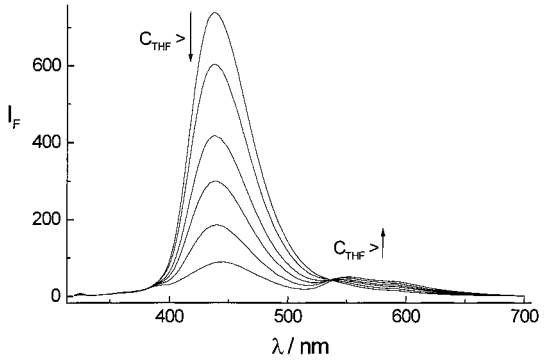

Figure 6. Changes in the fluorescence spectrum of HMMQ in CH_2Cl_2/THF when the concentration of THF is varied in the solution of HMMQ and *T* is held constant.

HMMQ to a 1,4-dioxane molecule because 7-HQ is the photoactive chromophore in HMMQ. Therefore, the formation of both Ω* and Z* must involve ESIPT to atom N2. Because Ω* and Z* are kinetically independent of each other, they must be formed along pathways that are kinetically not connected. In other words, X* leads merely to Ω* and does not yield Z*. The latter must be formed from a different type of excited enol form, which we shall refer to as Y*.

The ratio I_Z/I_K of the heights of the bands F_Z and F_K has previously been reported to depend on $1/C_S$ when the concentration C_S of 1,4-dioxane in the solvent mixture is varied.[17] Therefore a 1,4-dioxane molecule from the solvent mixture must participate in the formation of K*.

The form Z* must exist in a condition that inhibits the transformation into K* completely. It has been reported previously that position of the band F_Z of solutions of HMMQ in a number of neat solvents depends on the nature of the solvent and cannot be correlated with the dielectric constant. This result indicates specific interactions of Z* with solvent molecules such as 1,4-dioxane, diethyl ether, THF, and CH_2Cl_2.[18] In the case of solutions of HMMQ containing one of these proton-accepting solvents, such a proton-accepting solvent molecule (S) must appear in both the route to Ω* and Z*.

Upon cooling of the solution of HMMQ in *n*-hexane/5% 1,4-dioxane or in *n*-hexane/5% THF or in neat THF, the height of the band F_Z increases and in the former two cases an isoemissive point appears on the blue edge of the band (Figures 4 and 5). An isoemissive point appears on the red edge of the band when the concentration of THF is varied in the solution of HMMQ in CH_2Cl_2/THF, while *T* is constant (Figure 6). Later on, spectral evidence for the formation of complexes of oxygen and HMMN will be presented. Complexes of oxygen and HMMQ are therefore to be expected. The observed increase in fluorescence intensity cannot be attributed to a reduction in the efficiency of quenching by oxygen, because the quenching must be considered to be static when the fluorescence decay rate constant ($\sim 2.5 \times 10^9$ s^{-1}) and oxygen concentrations of $<10^{-3}$ M are taken into account. The concentration of complexes consisting of the solute and oxygen must increase on lowering *T*, and this change would cause more efficient fluorescence quenching, contrary to what is observed.

SCHEME 1. Conversion of excited species generated by photoexcitation of an equilibrium mixture of bare HMMQ (Y) and its complex (X) with a solvent molecule (S).

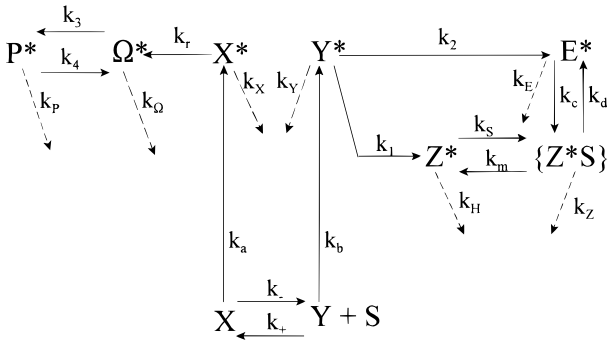

The facts just mentioned are taken into account in the design of Scheme 1. The excited keto form is represented as P* rather than as K* to keep a clear distinction in the notation between

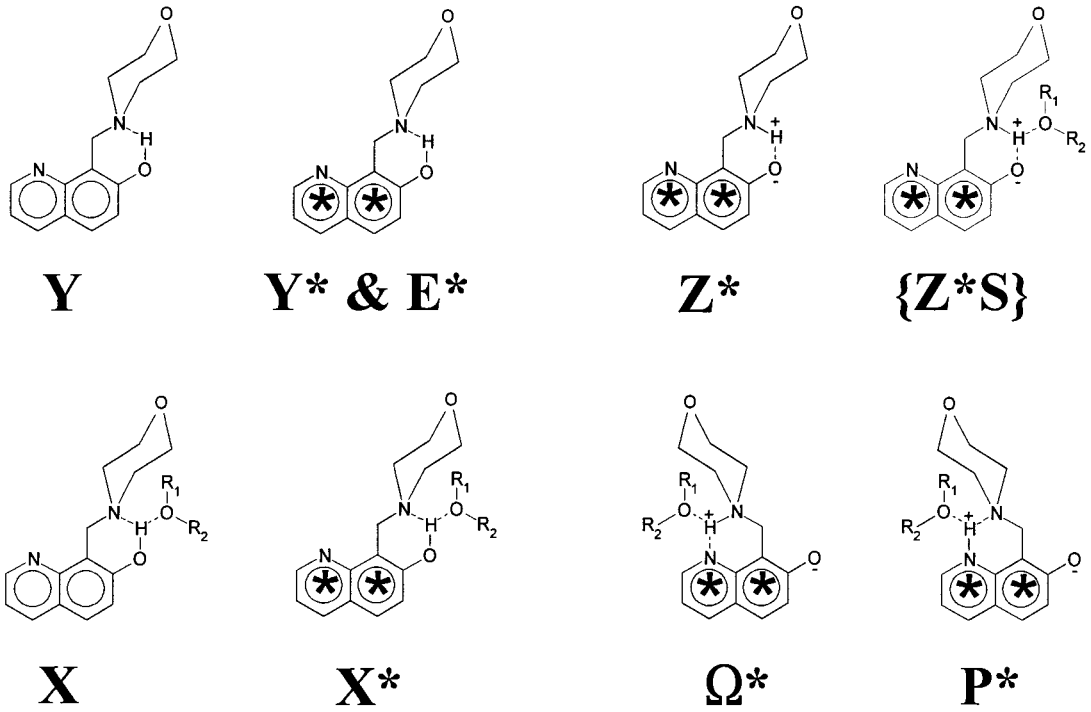

Figure 7. Chemical structures of the species appearing in Scheme 1. Structures with marked aromatic rings represent electronically excited species. X* and {Z*S} have the same structure, but X* is vibrationally excited and {Z*S} is vibrationless.

rate constants, equilibrium constants, and type of species. The rate at which excited states are prepared is determined by rate constants k_a and k_b, which are proportional to radiation density and transition probabilities of ground-state species X and Y, respectively. The constants k_Y, k_H, k_Z, k_E k_X, k_Ω, and k_P represent the total rate constant for decay of the associated species along all routes other than the path followed in their chemical conversion. The chemical structures of the species appearing in this scheme are shown in Figure 7. Excitation of X and Y with light of the same wavelength prepares Y* with less excess internal energy than X* because the formation of the complex of HMMQ will shift the first electronic absorption band of HMMQ to the red. Scheme 1 is based on the assumption that the excess energies in X* and Y* are much larger than k_BT and are needed to overcome an energy barrier in the first ESIPT step in HMMQ. Note that {Z*S} does not get converted into Ω*, despite its additional intermolecular H bond. The reason for this result is that the optical excitation prepares X* with sufficient excess energy to have some of it available for breaking of the intramolecular H bond after the first ESIPT step, implying that these processes must be faster than vibrational relaxation. After the first ESIPT step in Y*, the newly formed species Z* has insufficient excess energy available for breaking of the intramolecular bond. Species Z* relaxes vibrationally and forms a complex {Z*S} that does not get converted into K*. The band F_Z is now attributed to fluorescence from {Z*S}. Species Y* is allowed to relax vibrationally in competition with ESIPT. Vibrationally relaxed Y* is represented as E*. Species E* cannot make the first ESIPT step because it lacks sufficient internal energy. To account for the fact that the spectral position of the band F_E does not shift significantly when the solvent mixture *n*-hexane/1,4-dioxane gets richer in 1,4-dioxane, E* is supposed to remain in its bare form.

The general Scheme 1 has to be adjusted to reproduce all the experimental facts. This adjustment will be achieved by deriving expressions for the concentration (C_J) of each of the excited species (J) appearing in the scheme under stationary and pulse optical excitations and by considering when the C_J values agree with experiment. Species generated by excitation of Y will be treated before those arising from X.

Concentration of Excited Species in Scheme 1 under Stationary Illumination or on Pulse Excitation. *A. Temperature Dependence of the Peak Height of Fluorescence Band F_Z.* The concentrations of the excited species, generated from Y under the condition of weak stationary illumination that does not perturb the ground-state populations, are, according to Scheme 1,

$$C_{Y^*} = \frac{k_b}{k_1 + k_2 + k_Y} C_Y \tag{3}$$

$$C_{E^*} = \frac{1}{D}\{-[k_S(k_d + k_Z) + k_H(k_d + k_Z + k_m)]\alpha - k_d(k_S + k_H)\beta\} \tag{4}$$

$$C_{Z^*} = \frac{1}{D}\{-k_c k_m \alpha - [k_c(k_Z + k_m) + k_E(k_d + k_Z + k_m)]\beta\} \tag{5}$$

$$C_{\{Z^*S\}} = \frac{1}{D}\{-k_c(k_S + k_H)\alpha - k_S(k_c + k_E)\beta\} \tag{6}$$

with

$$\alpha \equiv \frac{k_2 k_b}{k_1 + k_2 + k_Y} C_Y \qquad \beta \equiv \frac{k_1 k_b}{k_1 + k_2 + k_Y} C_Y \tag{7}$$

$$D \equiv -k_m k_H(k_c + k_E) - k_Z k_c(k_S + k_H) - k_E(k_d + k_Z)(k_S + k_H) \tag{8}$$

The time dependence of the band F_Z, discussed in the next section, leads to the conclusion $k_d = 0$, when agreement with experiment is to be obtained. Here, one has to take also $k_c = 0$ to reproduce the experimental dependence of the peak intensity of F_Z on T. Using $k_c = 0$ and $k_d = 0$ one obtains

$$D = -k_E\{k_H(k_m + k_Z) + k_S k_Z\} \quad (9)$$

$$C_{E^*} = \left\{\frac{k_b k_2}{(k_1 + k_2 + k_Y)}\right\}\left\{\frac{1}{k_E}\right\}C_Y \quad (10)$$

$$C_{Z^*} = \left\{\frac{k_b k_1}{(k_1 + k_2 + k_Y)}\right\}\left\{\frac{(k_m + k_Z)}{k_H(k_m + k_Z) + k_S k_Z}\right\}C_Y \quad (11)$$

$$C_{\{Z^*S\}} = \left\{\frac{k_b k_1}{(k_1 + k_2 + k_Y)}\right\}\left\{\frac{k_S}{k_H(k_m + k_Z) + k_S k_Z}\right\}C_Y \quad (12)$$

Because the observed growth of the fluorescence F_Z is orders of magnitude faster than its decay, the term k_Y in the denominator of the first factor in eqs 10 and 12 and the term $k_H\, k_Z$ in the denominator of the second factor in eq 12 may be neglected. These approximations yield

$$C_{E^*} = \left\{\frac{k_b k_2}{(k_1 + k_2)}\right\}\left\{\frac{1}{k_E}\right\}C_Y \quad (13)$$

$$C_{\{Z^*S\}} = \left\{\frac{k_b k_1}{(k_1 + k_2)}\right\}\left\{\frac{k_S}{k_H k_m + k_S k_Z}\right\}C_Y \quad (14)$$

Provided that the first factor between brackets does not depend on T, a simple exponential temperature dependence arises from eq 14 when $k_S\, k_Z \gg k_H\, k_m$. The condition applies to the situation in which the amount of Z* is negligible in the interconversion of Z* and {Z* S} or in practical terms when $k_m = 0$. Under these circumstances, eq 14 reduces to

$$C_{\{Z^*S\}} = G_{\{Z^*S\}}C_Y \text{ with } G_{\{Z^*S\}} \equiv \left\{\frac{k_b k_1}{(k_1 + k_2)}\right\}\left\{\frac{1}{k_Z}\right\} \quad (15)$$

Equation 15 explains the dependence of the intensity of band F_Z on T observed in the case of the solution of HMMQ in *n*-hexane/5% 1,4-dioxane, in *n*-hexane/5% THF, and in neat THF. When the logarithm of the height of the band F_Z is plotted as a function of $1/T$, a linear relation is revealed (Figure 8). This result means that the central part of the band F_Z must arise predominantly from a single type of species. In Scheme 1, this species is obviously {Z*S}. The observed linear relation must follow from eq 15, provided that C_Y does not change noticeably in the temperature range. The undetectable change in the ground-state equilibrium will be dealt with in more detail later on when more insight in the matter will be available. Denoting the wavelength of the maximum of band F_Z by λ_{Zm} and the radiative rate constant as $k_{fZ}(\lambda_{Zm})$ and using the Arrhenius form $k_Z = A_Z \exp(-\epsilon_Z/k_B T)$, one gets

$$I_Z(\lambda_{Zm}) = k_{fZ}(\lambda_{Zm})C_{\{Z^*S\}} = k_{fZ}(\lambda_{Zm})\left\{\frac{k_b k_1}{(k_1 + k_2)}\right\}\left\{\frac{C_Y}{A_Z}\right\}\exp\left(\frac{\epsilon_Z}{k_B T}\right) \quad (16)$$

which produces a straight line with positive slope when plotted as a function of $1/T$, as in Figure 8. One may conclude that k_Z is determined by a single decay process. The validity of eq 16 implies that k_1 is independent of T. This result agrees with the suggestion that the process leading from Y* to Z* involves tunneling and not thermal barrier crossing of the proton. In Table 1, the activation energies derived from the plots in Figure 8 are also listed. In the case of a solution of HMMQ in *n*-hexane/5% 1,4-dioxane, $\epsilon_Z = 530$ cm^{-1} is obtained. Within experimental accuracy this value is equal to that for the activation energy E_a (526 cm^{-1}) of γ_Z (Table 1) and is in striking agreement with

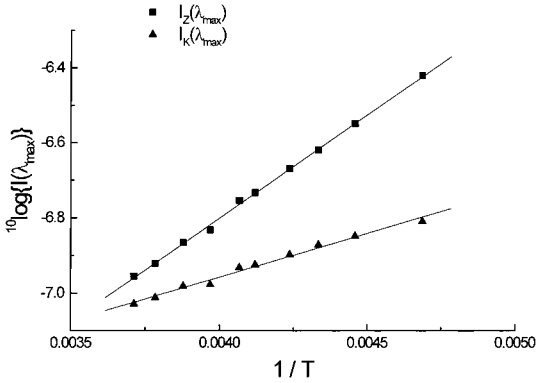

Figure 8. Temperature dependence of the height of the band F_Z of HMMQ in *n*-hexane/5% 1,4-dioxane, in *n*-hexane/5% THF, and in neat THF, and also of the height of the band F_K in the latter case.

the identification of rate constant γ_Z with k_Z. The observed increase in height of the band F_Z with decreasing T can now be attributed to the diminishing magnitude of the rate constant k_Z for the radiationless decay of {Z*S}, because its fluorescence quantum yield is practically equal to k_{fZ}/k_Z .

The process dominating k_Z may be identified with thermally activated intersystem crossing because then the observed variation of the magnitude of ϵ_Z with the solvent composition may be understood. Apparently, spin−orbit coupling of a vibrationally excited substate of the fluorescent singlet state of {Z*S} with a (nearly) resonant state in the triplet manifold is needed to achieve intersystem crossing. The variation of the energy gaps between states in the singlet and triplet manifolds depend both on the strength of the intermolecular H bond in the complex {Z*S} and on bulk solvent polarization. This dependence makes the variation of energy gaps and therefore the variation of ϵ_Z unpredictable with currently feasible quantum chemical calculations.

The disappearance of the band F_E and the attenuation of the intensity of the band F_Z with increasing C_S fits in Scheme 1 as a direct consequence of the ground-state equilibrium. With increasing C_S, there is less Y available to generate Y* and therefore less Z* and {Z*S} appear.

The solvent effect on the spectral position of the band F_Z indicates that solvent molecules with a large localized negative charge maintain an H bond between the atom with this charge and the proton on atom N1 in Z*. A crude explanation of the spectral shift is that appreciable shifts in band position may be caused by the intramolecular Stark effect on the electronic states of the π-electron system, arising from the combined electric fields of the proton and the negative solvent charge in its vicinity. The compensation of the field of the proton in the Stark effect depends on both the magnitude of the negative solvent charge and on its distance to the proton. The distance of closest approach may be limited by steric factors. This situation seems to occur when S represents diethyl ether because the spectral shift is then smaller than when S stands for 1,4-dioxane, despite the smaller dielectric constant and proton acceptor strength in the case of 1,4-dioxane. The Stark effect picture is supported by a molecular dynamics simulation of the electric field at the center of a 1,3-dioxane molecule embedded in liquid 1,4-dioxane, which reveals that the field at the dipolar solute arises nearly completely from the charges on the atoms of 1,4-dioxane, which are the nearest neighbors of the solute.[20] The bulk of liquid 1,4-dioxane contributes just a little bit to the field. Such a state of affair is also expected in the case of {Z*S} in *n*-hexane/1,4-dioxane mixtures. However, the fine-tuning of energy gaps between closely spaced singlet and triplet excited states caused

by the bulk contributions to the field across the π-electron system of Z* in {Z*S} may have severe consequences for the rate constant for intersystem crossing. This fine tuning seems to explain the observed behavior of γ_Z as a function of the concentration of 1,4-dioxane in the solvent. A more refined explanation of the perturbation of the states of the bare solute by H bonding to a solvent must be based on rather accurate quantum mechanical calculations of the electronic states of the complex, allowing redistribution of electron density over both solvent and solute molecule. This task is time-consuming on a super computer, which has to wait for favorable opportunities.

Dependence of the Ratio of Bands F_Z and F_K on C_S and Height of Band F_K as a Function of T. The following expressions are derived for the concentrations of species in the section on the left-hand side of Scheme 1, under conditions of weak stationary illumination:

$$C_{X^*} = \frac{k_a}{k_r + k_X} C_X \tag{17}$$

$$C_{\Omega^*} = \left\{\frac{k_a k_r}{k_r + k_X}\right\}\frac{k_4 + k_P}{N} C_X \tag{18}$$

$$C_{P^*} = G_P C_X \text{ with } G_P \equiv \left\{\frac{k_a k_r}{k_r + k_X}\right\}\frac{k_3}{N} \tag{19}$$

with

$$N \equiv (k_3 + k_\Omega)(k_4 + k_P) - k_3 k_4 = k_\Omega(k_4 + k_P) + k_3 k_P \tag{20}$$

Recall that the bands F_Z and F_K are attributed to fluorescence of species {Z*S} and P* in Scheme 1. Using eqs 15 and 19 for $C_{\{Z^*S\}}$ and C_{P^*}, respectively, the intensities of $F_Z(\lambda_{Zm})$ and $F_K(\lambda_{Km})$ at the maxima of the bands F_Z and F_K respectively can be calculated as follows:

$$\frac{I_Z(\lambda_{Zm})}{I_K(\lambda_{Km})} = \frac{I_{\{ZS\}}(\lambda_{Zm})}{I_P(\lambda_{Pm})} = \frac{k_{f\{ZS\}}(\lambda_{Zm})G_{\{ZS\}}}{k_{fP}(\lambda_{Pm})G_P}\frac{C_Y}{C_X} = \frac{k_{f\{ZS\}}(\lambda_{Zm})G_{\{ZS\}}}{k_{fP}(\lambda_{Pm})G_P K_{eq}}\frac{1}{C_S} \tag{21}$$

where $k_{fZ}(\lambda_{Zm})$ and $k_{fP}(\lambda_{Pm})$ are the rate constant for photoemission at the specified wavelength by {Z*S} and P*, respectively, and K_{eq} is the equilibrium constant for the ground-state equilibrium involving X and Y. The concentration dependence of the intensity ratio in eq 21 agrees with the experimental result just mentioned.

Figure 8 reveals also the T dependence of the height of the band F_K in the case of a solution of HMMQ in neat THF. The observed behavior must follow from a special case of eq 19. The magnitude of k_X must be comparable with the decay rate constant of the band F_E and, based on the previous discussion, can be assigned a value of $\sim 10^9$ s^{-1}. This value is certainly an order of magnitude smaller than the rate constant for the growth of the band F_K. Therefore k_X can be neglected in eq 19. When in addition, $k_3, k_4 \gg k_\Omega, k_P$ is taken into account, the resulting expression still does not reproduce the behavior shown in Figure 8. The term $k_4 k_\Omega$ must vanish in the denominator of the simplified expression for G_P to get the desired behavior. The resulting expression for the fluorescence from P* at λ_{Pm} is then

$$I_P(\lambda_{Pm}) = k_{fP}(\lambda_{Pm})C_{P^*} = k_{fP}(\lambda_{Pm})k_a\left\{\frac{1}{k_P}\right\}C_X \tag{22}$$

Introducing an Arrhenius T dependence of k_P as $k_P = A_P \exp(-\epsilon_P/k_B T)$ results in

$$I_{P^*}(\lambda_{Pm}) = k_{fP}(\lambda_{Pm})C_{P^*} = \frac{k_{fP}(\lambda_{Pm})k_a C_X}{A_P}\exp\left(\frac{\epsilon_P}{k_B T}\right) \tag{23}$$

To reproduce the linear log I_{K^*} versus T^{-1} plot, C_X must remain constant. Because P* represents K* in Scheme 1, one obtains ϵ_K (in Table 1) from the plot. The comparison of this value with the magnitude of E_a in γ_{K2} will be presented in the next section.

Time Dependence of the Fluorescence of the Bands F_E, F_Z, and F_K on Pulse Excitation. So far, the T dependence of the peak height of the band F_Z of HMMQ led to the conclusion that k_c, k_d, and k_m in Scheme 1 have to be set equal to zero. It is worthwhile to see if these conditions follow also from analysis of the time dependence of the band F_Z . Because only a decaying component is detected in the time dependence of the band F_Z, its growth must be too fast to be detectable, which means that k_1 and k_S are both $> 2 \times 10^{11}$ s^{-1}. The growth of the band F_E of HMMQ in *n*-hexane/1,4-dioxane mixtures can also not be resolved. In the analysis of the observed time dependence, the species E* and {Z*S} may therefore be considered to have been prepared by direct excitation. The kinetic system to be analyzed may then be represented as in Scheme 2 with the conditions $C_{E^*}(t = 0) > 0$ and $C_{\{Z^*S\}}(t = 0) > 0$. The time dependence of C_{E^*} and $C_{\{Z^*S\}}$ are then given by

$$C_E(t) = -\frac{\{\rho_1 + (k_d + k_Z)A + k_d B\}}{D}e^{\rho_1 t} + \frac{\{\rho_2 + (k_d + k_Z)A + k_d B\}}{D}e^{\rho_2 t} \tag{24}$$

$$C_{\{Z^*S\}}(t) = -\frac{\{\rho_1 + (k_c + k_E)B + k_c A\}}{D}e^{\rho_1 t} + \frac{\{\rho_2 + (k_c + k_E)B + k_c A\}}{D}e^{\rho_2 t} \tag{25}$$

with

$$2\rho_1 = -(k_c + k_d + k_E + k_Z) - D \tag{26}$$

$$2\rho_2 = -(k_c + k_d + k_E + k_Z) + D \tag{27}$$

$$D \equiv \sqrt{(k_c + k_d + k_E + k_Z)^2 - 4\{(k_c + k_E)(k_d + k_Z) - k_c k_d\}} \tag{28}$$

$$A \equiv C_E(t = 0) \qquad B \equiv C_{\{Z^*S\}}(t = 0) \tag{29}$$

Single-exponential decay of {Z*S} will be predicted by eq 25 when k_c and k_d are both much $> k_E$ and k_Z. This situation yields the approximations $\rho_1 = -(k_c + k_d)$ and $\rho_2 = -1/2(k_E + k_Z)$. However, ρ_2 will still not exhibit Arrhenius behavior as a function of T in general. The desired behavior is obtained when $k_d = 0$ in eqs 26 and 27. These equations then yield

$$\rho_1 \approx -(k_c + k_E) \tag{30}$$

$$\rho_2 \approx -k_Z \tag{31}$$

Now the second term in eq 24 vanishes and C_{E^*} decays monoexponentially with rate constant $(k_c + k_E)$ while $C_{\{Z^*S\}}$ grows with the same rate constant and decays with rate constant

SCHEME 2. Interconversion and decay of the excited bare enol form E* and the excited complex {Z*S} of the zwitterionic form of HMMQ, which retain a link between the morpholino group and the O atom on the aromatic ring and which have been prepared virtually by direct excitation.

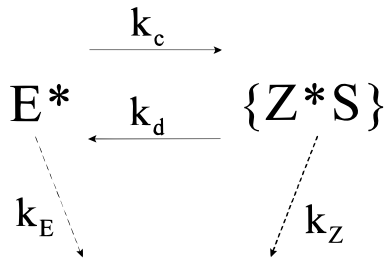

k_Z. Note that analysis of the time dependence shows that k_d, but not k_c, has to vanish in Scheme 1 to get agreement with experiment.

It may now be clear that Scheme 1 can explain the monoexponential decay of the intensity I_Z, the Arrhenius behavior of γ_Z, and the spectral shifts of the band F_Z arising from specific solute−solvent interaction by attributing the band F_Z to fluorescence by species {Z*S}. The ordering of the magnitudes of the rate constants (Table 2) for the decay of the fluorescence F_E of 7-HQ in 1,4-dioxane (2.47×10^9 s^{-1}) and of the fluorescence F_Z of HMMQ in *n*-hexane (0.62×10^9 s^{-1}) and in 1,4-dioxane (1.34×10^9 s^{-1}) can be understood. The difference between the first two rate constants may be attributed to the stronger H bond with the deprotonated excited quinoline moiety in the latter case. Because the additional H bond with a solvent molecule weakens the intramolecular H bond, the magnitude of k_Z is expected to lie between its values when either only an intermolecular (7-HQ in 1,4-dioxane) or only an intramolecular H bond (HMMQ in *n*-hexane) is involved.

A magnitude $k_S \gg 2 \times 10^{11}$ s^{-1} is not expected to be encountered for very small values of C_S, but may be observed when, for example, $C_S > 10^{-1}$ M and when the neat solvent S is used to prepare the sample. In the latter cases, the attachment of a solvent molecule to Z* must be a cage reaction requiring merely a single encounter of the reactants to have $k_S \gg 10^{11}$ s^{-1}.

In Scheme 1, X* is converted into Ω*, which then yields P* in a reversible reaction. In contrast to the fluorescence in band F_Z, the growth of the fluorescence in band F_K can be observed because the rate of growth is limited by the rotational Brownian motion of the side group in HMMQ, which is relatively slow. The time dependence of the concentrations of the three species, appearing after excitation of X with a short pulse, has to be described as a sum of three exponential functions of time. Using the initial conditions

$$C_{X*}(t=0) \equiv A \qquad C_{\Omega*}(t=0) = 0 \qquad C_{P*}(t=0) = 0 \quad (32)$$

the following expression is obtained for $C_{P*}(t)$:

$$C_{P*} = \left\{\frac{[k_r k_3]A}{(\vartheta_1 - \vartheta_2)(\vartheta_1 - \vartheta_3)}\right\} e^{\vartheta_1 t} + \left\{\frac{[k_r k_3]A}{(\vartheta_2 - \vartheta_1)(\vartheta_2 - \vartheta_3)}\right\} e^{\vartheta_2 t} + \left\{\frac{[k_r k_3]A}{(\vartheta_3 - \vartheta_1)(\vartheta_3 - \vartheta_2)}\right\} e^{\vartheta_3 t} \quad (33)$$

with

$$\vartheta_1 = -(k_X + k_r) \quad (34)$$

$$2\vartheta_2 = -(k_\Omega + k_P + k_3 + k_4) - D_L \quad (35)$$

$$2\vartheta_3 = -(k_\Omega + k_P + k_3 + k_4) + D_L \quad (36)$$

$$D_L \equiv \sqrt{(k_\Omega + k_P + k_3 + k_4)^2 - 4(k_\Omega k_P + k_3 k_P + k_4 k_\Omega)} \quad (37)$$

When k_3 and k_4 are much larger than k_Ω and k_P, the rate constants J_2 and J_3 may be approximated by

$$\vartheta_2 = -(k_3 + k_4) \quad (38)$$

$$\vartheta_3 = -\frac{1}{2}(k_\Omega + k_P) \quad (39)$$

Which leads to the following approximation:

$$C_{P*} \approx \left\{\frac{[k_r k_3]A}{(-\vartheta_1 \vartheta_2)}\right\} e^{\vartheta_1 t} + \left\{\frac{[k_r k_3]A}{(\vartheta_2^2)}\right\} e^{\vartheta_2 t} + \left\{\frac{[k_r k_3]A}{(\vartheta_1 \vartheta_2)}\right\} e^{\vartheta_3 t} \quad (40)$$

Because the denominator of the second term in eq 40 gets very large, the amplitude of this term gets small compared with the two other terms and becomes undetectable. Retaining the first and third term in eq 40, one gets

$$C_{P*} \approx -\left\{\frac{[k_r k_3]A}{(k_X + k_r)(k_3 + k_4)}\right\} e^{-(k_X + k_r)t} + \left\{\frac{[k_r k_3]A}{(k_X + k_r)(k_3 + k_4)}\right\} e^{-1/2(k_\Omega + k_P)t} \quad (41)$$

where the first and second term represent the growth and the decay of the band F_K, respectively. Comparison of eqs 2 and 41 leads to

$$A_{K1} = -\left\{\frac{[k_r k_3]A}{(k_X + k_r)(k_3 + k_4)}\right\} < 0 \quad (42)$$

$$\gamma_{KI} = (k_X + k_r)$$

$$A_{K2} = \left\{\frac{[k_r k_3]A}{(k_X + k_r)(k_3 + k_4)}\right\} > 0 \quad (43)$$

$$\gamma_{K2} = \frac{1}{2}(k_\Omega + k_P)$$

In practice γ_{K1} and γ_{K2} are of the same order of magnitude. To reproduce this and the Arrhenius behavior of γ_{K1} and γ_{K2}, each of them must depend on a single rate constant. Because γ_{K1} is known to depend strongly on solvent friction,[14−18] k_r must show up in the expression for γ_{K1}. The desired growth of the band F_K emerges from eq 41, when $k_X \ll k_r$; namely,

$$\gamma_{KI} \approx k_r \quad (44)$$

and the desired decay of this band follows eq 43 if either k_Ω or k_P disappear on the right-hand side of this equation. The ground on which the choice can be based is that ϵ_K for the solution of HMMQ in neat THF and E_a in γ_{K2} for a solution of HMMQ in *n*-hexane/5% 1,4-dioxane have magnitudes (Table 1) that are equal within experimental accuracy. This situation favors the choice

$$\gamma_{K2} = \frac{1}{2}k_P \quad (45)$$

TABLE 2: Effects of Deuteration of the OH Group on Rate Constants in the Dynamics of the Fluorescence of HMMQ, HMMN, and 7-HQ

solute	band	kinetics[a] $10^{-9}\ \gamma$(H)/[s^{-1}]	kinetics[b] $10^{-9}\ \gamma$(D)/[s^{-1}]	$\gamma(H)/\gamma(D)$
HMMQ in *n*-hexane	F_Z	$a(H)\exp\{-\gamma_Z(H)t\}$	$a(D)\exp\{-\gamma_Z(D)t\}$	
		$\gamma_Z(H) = 0.620 \pm 2\%$	$\gamma_Z(D) = 0.631 \pm 2\%$	0.98
HMMQ in 1,4-dioxane	F_Z	$a(H)\exp\{-\gamma_Z(H)t\}$	$a(D)\exp\{-\gamma_Z(D)t\}$	
		$\gamma_Z(H) = 1.324 \pm 1\%$	$\gamma_Z(D) = 1.322 \pm 1\%$	1.00
HMMQ in 1,4-dioxane	F_K	$a_{K1}(H)\exp\{-\gamma_{K1}(H)t\}$	$a_{K1}(D)\exp\{-\gamma_{K1}(D)t\}$	
		$+ a_{K2}(H)\exp\{-\gamma_{K2}(H)t\}$	$+ a_{K2}(D)\exp\{-\gamma_{K2}(D)t\}$	
		$a_{K1}(H) = -a_{K2}(H)$	$a_{K1}(D) = -a_{K2}(D)$	
		with $a_{K1}(H) < 0$	with $a_{K1}(D) < 0$	
		$\gamma_{K1}(H) = 1.675 \pm 3\%$	$\gamma_{K1}(D) = 1.915 \pm 4\%$	1.23
		$\gamma_{K2}(H) = 1.428 \pm 3\%$	$\gamma_{K2}(D) = 1.158 \pm 3\%$	0.87
7-HQ in 1,4-dioxane	F_E	$a(H)\exp\{-\gamma(H)t\}$	$a(D)\exp\{-\gamma(D)t\}$	
		$\gamma(H) = 2.472 \pm 1\%$	$\gamma(D) = 2.604 \pm 2\%$	0.95
HMMN in *n*-hexane	F_E	$a(H)\exp\{-\gamma(H)t\}$	$a(D)\exp\{-\gamma(D)t\}$	
		$\gamma(H) = 0.212 \pm 4\%$	$\gamma(D) = 0.194 \pm 4\%$	1.09
HMMN in 1,4-dioxane	$F_E + F_Z$	$a(H)\exp\{-\gamma(H)t\}$	$a(D)\exp\{-\gamma(D)t\}$	
		$\gamma(H) = 0.296 \pm 1\%$	$\gamma(D) = 0.330 \pm 1\%$	0.9

[a] Solutions are deoxygenated. [b] Solutions are deoxygenated and the OH group of the solute is deuterated

This choice means that ϵ_K does not depend as strongly on the solvent polarity as ϵ_Z, which is reasonable because the chromophoric system in K* is electrically neutral, whereas it is negatively charged in the case of {Z*S}. This choice also agrees with the spectral shift of the band F_K which is much smaller than that of the band F_Z when the solvent is changed (e.g., from neat 1,4-dioxane to neat THF).

Isoemissive Points in the Fluorescence Spectrum of HMMQ when the Temperature is Varied. The ground-state equilibrium between X and Y cannot cause the increase of intensity in the band F_Z with decreasing T because less Y would be available to produce {Z*S} at lower T. This situation rules out the possibility that the appearance of an isoemissive point is due to the T dependence of this equilibrium. The condition to find such an isoemissive point at λ_B is

$$I(\lambda_B) = k_{fE}(\lambda_B)C_{E^*} + k_{f\{ZS\}}(\lambda_B)C_{\{Z^*S\}} = \xi' = constant \tag{46}$$

where $k_{fE}(\lambda_B)$ and $k_{f\{ZS\}}(\lambda_B)$ are radiative rate constants for fluorescence of E* and {Z*S}at wavelength λ_B, respectively. Applying eqs 13 and 14, this condition yields

$$k_{fE}(\lambda_B)\left(\frac{k_b}{k_1+k_2}\right)\left(\frac{k_2}{k_E}\right)C_Y + k_{f\{ZS\}}(\lambda_B)\left(\frac{k_b}{k_1+k_2}\right)\left(\frac{k_1}{k_Z}\right)C_Y = \xi' \tag{47}$$

Dividing both sides of eq 46 by the factor k_b one obtains

$$\frac{k_{fE}(\lambda_B)}{k_E}\left(\frac{k_2}{k_1+k_2}\right)C_Y + \frac{k_{f\{ZS\}}(\lambda_B)}{k_Z}\left(\frac{k_1}{k_1+k_2}\right)C_Y = \xi = constant \tag{48}$$

$$\frac{k_{fE}(\lambda_B)}{k_E}k_2C_Y + \frac{k_{f\{ZS\}}(\lambda_B)}{k_Z}k_1C_Y = \xi k_1 + \xi k_2 \tag{49}$$

$$\frac{k_{fE}(\lambda_B)}{k_E} = \frac{k_{f\{ZS\}}(\lambda_B)}{k_Z} = \frac{\xi}{C_Y} \tag{50}$$

Introducing the equilibrium constant K_{eq} of the ground-state equilibrium between Y + S and X and the combined concentrations C_0 of X and Y, eq 50 can be written as

$$\frac{k_{fE}(\lambda_B)}{k_E} = \frac{k_{f\{ZS\}}(\lambda_B)}{k_Z} = \frac{\xi C_0}{1 + K_{eq}C_S} \tag{51}$$

Two limiting cases of eq 51 may be analyzed further; namely, when $K_{eq}C_S \ll 1$ and $K_{eq}C_S \gg 1$. The condition $K_{eq}C_S \ll 1$ leads to

$$\frac{k_{fE}(\lambda_B)}{k_E} = \frac{k_{f\{ZS\}}(\lambda_B)}{k_Z} = \xi C_0 \tag{52}$$

and $K_{eq}C_S \gg 1$ yields

$$\frac{k_{fE}(\lambda_B)}{k_E} = \frac{k_{f\{ZS\}}(\lambda_B)}{k_Z} = \frac{\xi C_0}{K_{eq}C_S} \tag{53}$$

Equations 52 and 53 do not provide a relation that is independent of T. Under very special conditions, one may obtain a T-independent relation to be satisfied for an isoemissive point. These conditions may be revealed by taking the T dependence of k_E, k_Z, and K_{eq} into account and writing

$$k_E = A_E\exp\left(\frac{-\epsilon_E}{k_BT}\right) \qquad k_Z = A_Z\exp\left(\frac{-\epsilon_Z}{k_BT}\right)$$

$$K_{eq} = A_{eq}\exp\left(\frac{-\epsilon_{eq}}{k_BT}\right) \tag{54}$$

Equations 52 and 53 yield a T-independent relation if $\epsilon_E = \epsilon_Z$ and $\epsilon_E = \epsilon_Z = \epsilon_{eq}$ holds, respectively. The practical meaning of these conditions is that the differences between ϵ_E, ϵ_Z, and ϵ_{eq} are too small compared with k_BT to be resolved in the experiment. The analysis of the T dependence of the height of the bands F_Z and F_K revealed that variations in C_Y and C_X as a function of T are not detectable in the limited range $258 < T < 300$ K. Let us see whether this situation may help to choose between the possibilities $K_{eq}C_S \ll 1$ and $K_{eq}C_S \gg 1$.

$$\frac{dC_X}{dT} = -\frac{dC_Y}{dT} = C_0C_S\left\{\frac{K_{eq}}{(1+K_{eq}C_S)^2}\right\}\frac{\epsilon_{eq}}{k_BT^2}$$

$$\text{with } C_0 \equiv C_Y + C_X \tag{55}$$

$$\frac{\Delta C_X}{C_X} = \frac{\epsilon_{eq}}{k_BT}\left\{\frac{1}{(1+K_{eq}C_S)}\right\}\frac{\Delta T}{T} \tag{56}$$

$$\frac{\Delta C_Y}{C_Y} = -\frac{\epsilon_{eq}}{k_BT}\left\{\frac{K_{eq}C_S}{(1+K_{eq}C_S)}\right\}\frac{\Delta T}{T} \tag{57}$$

Consider solutions of HMMQ exhibiting an isoemissive point on the blue edge of the band F_Z. If in those cases $K_{eq}C_S \gg 1$

holds, then $\epsilon_E = \epsilon_Z = \epsilon_{eq}$ has to be satisfied. Because ϵ_{eq}/k_BT is > 1 and $\Delta T/T$ is ~0.1, the condition $K_{eq}C_S \gg 1$ would imply a variation of >10% in C_Y, which is in contradiction with the condition that the variation in C_Y is not detectable when an isoemissive point appears on the blue edge of F_Z during variation of T. In those cases, the condition $K_{eq}C_S \ll 1$ must therefore hold. When $K_{eq}C_S \ll 1$, the variation in C_X is >10% and therefore an isoemissive point on the red edge of the band F_Z is not to be expected when T is varied. This expectation agrees with the fact that none of the solutions show isoemissive points on both the blue and red edge of the band F_Z when T is varied. The sample of HMMQ in *n*-hexane/5% THF allows a larger range for the variation of T, but the isoemissive point on the blue edge of the band F_Z (Figure 5) is only sharply defined when the range of temperatures is limited between 30 and −15 °C, as in the case of the solution in *n*-hexane/5% 1,4-dioxane. If the full range of temperatures is considered in the plot, the isoemissive point smears out. This result implies that C_Y does not change significantly within the limited temperature range, but is not constant over the broader range.

The solution of HMMQ in neat THF shows neither an isoemissive point on the blue edge nor on the red edge of the band F_Z when T is varied. The lack of the isoemissive point at the blue side may be considered to mean that this solution satisfies the condition $K_{eq}C_S \gg 1$, because this also explains that the band F_E disappeared completely in this case.

Isoemissive Point in the Fluorescence Spectrum of HMMQ When the Concentration of the Component Acting as Proton Acceptor in the Solvent Mixture is Varied. The isoemissive point on the red edge of the band F_Z in the series of solutions of HMMQ in CH_2Cl_2/THF (Figure 6) can be attributed to overlap of the bands F_Z and F_K. The condition to find such an isoemissive point at λ_R is

$$I(\lambda_R) = k_{f\{ZS\}}(\lambda_R)C_{\{Z^*S\}} + k_{fP}(\lambda_R)C_{P^*} = \zeta = \text{constant} \quad (58)$$

$$I(\lambda_R) = \{k_{f\{ZS\}}(\lambda_R)G_{\{ZS\}}\}C_Y + \{k_{fP}(\lambda_R)G_P\}C_X = \zeta \quad (59)$$

$$I(\lambda_R) = \{k_{f\{ZS\}}(\lambda_R)G_{\{ZS\}}\}\frac{C_0}{(1 + K_{eq}C_S)} + \{k_{fP}(\lambda_R)G_P\}\frac{K_{eq}C_0C_S}{(1 + K_{eq}C_S)} = \zeta \quad (60)$$

The condition is satisfied when

$$k_{f\{ZS\}}(\lambda_R)G_{\{ZS\}}C_0 = k_{fP}(\lambda_R)G_PC_0 = \zeta \quad (61)$$

The condition in eq 61 may be met, provided that the rate constants in the quantities $G_{\{ZS\}}$ and G_P do not change in the course of the variation of C_S as a result of solute−solvent interactions. The appearance of the isoemissive point means therefore that k_3 does not change in the range of variations of C_S.

Effects of Oxygen and Deuteration of the OH Group in 7-HQ, HMMN, and HMMQ. The fluorescence of 7-HQ, HMMN, and HMMQ is quenched by oxygen. Therefore, the samples had been thoroughly deoxygenated in the studies of the changes in the fluorescence behavior caused by deuteration of the OH group. The deoxygenation of solutions in 1,4-dioxane causes substantially smaller changes in the fluorescence intensity of the solute than in the case of *n*-hexane as solvent. The reason for this result is that 1,4-dioxane had already been deoxygenated by reaction of oxygen with sodium when it refluxed and that only a small amount of oxygen got into the solution during sample preparation. Figure 9 shows small but significant changes

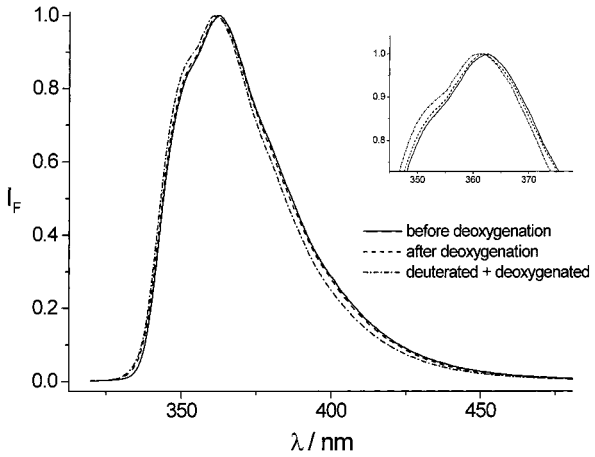

Figure 9. Effect of oxygen and deuteration on the fluorescence spectrum of HMMN in *n*-hexane.

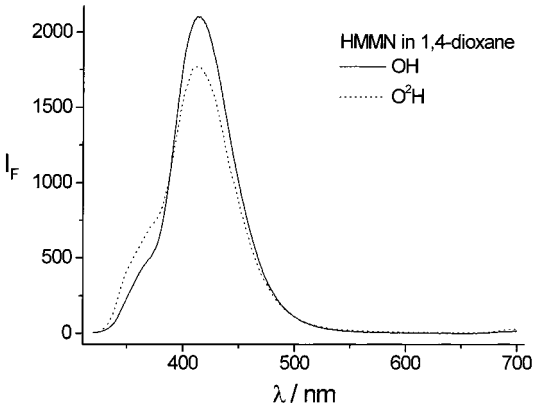

Figure 10. Loss in intensity of band F_Z and gain in intensity of band F_E of HMMN in 1,4-dioxane resulting from deuteration.

in the fluorescence spectrum of HMMN in *n*-hexane caused by deoxygenation of the sample and by deuteration of the solute. Similar effects of oxygen have not been observed in the other samples studied. The large spectral changes arising when the solvent for HMMN is changed from *n*-hexane to 1,4-dioxane (Figure 10) indicates that the band F_Z is absent in the former case. The slight blue shift of the band (F_E) on removal of oxygen in the solution of HMMN in *n*-hexane may be attributed to the disappearance of the complex between HMMN and oxygen from the sample. The much larger blue shift arising from deuteration indicates that there is emission from a thermally excited vibrational level (at 300 K) whose frequency is sensitive to deuteration.

Table 2 shows to that extent rate constants in the dynamics of the fluorescence are modified by deuteration of the OH group in the ground-state molecules 7-HQ, HMMN, and HMMQ when they are dissolved in either neat *n*-hexane or in neat 1,4-dioxane. The rate constant γ_Z of HMMQ in *n*-hexane and in 1,4-dioxane does not change significantly due to the deuteration. This result is not surprising, because the proton or the deuteron in species {Z*S} does not have a covalent bond with the excited delocalized system of electrons in the complex. By contrast, the deuteration of HMMQ leads to substantially more intensity in the bands F_Z, F_E, and F_K (Figure 11) and also to significant kinetic isotope effects in γ_{K1} and γ_{K2}. The interpretation of the isotope effect on the intensities must be based on eqs 13, 15, and 21. Because the decay of the band F_Z is not affected by deuteration, the enhancement in its intensity must arise from an increase in the quantum yield for the formation of Z*, despite a reduction in the tunneling rate determining k_1. This increase

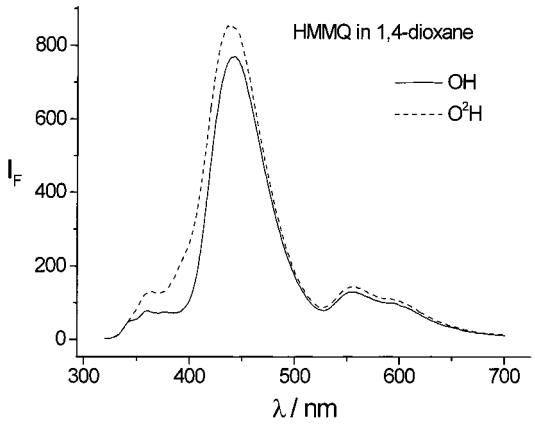

Figure 11. Gain in intensities of the fluorescence bands of HMMQ in 1,4-dioxane caused by deuteration. The spectra are corrected for differences in absorbance at the excitation wavelength.

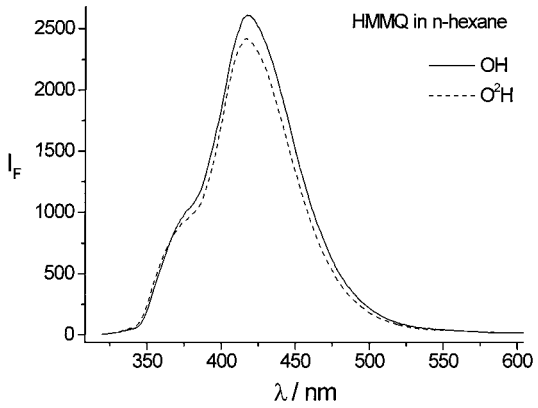

Figure 12. Loss of intensity in the main fluorescence band (F_Z) of HMMQ in *n*-hexane caused by deuteration. The spectra are corrected for differences in absorbance at the excitation wavelength.

can be attributed to a slower vibrational relaxation of the primary excited bare enol form (Y* in Scheme 1) when it is deuterated, because then formation of Z* is favored over the production of totally relaxed E*. The observation that the intensity of the band F_E is increasing nevertheless may be attributed to a reduction in the rate constant for intersystem crossing on deuteration. This explanation is reasonable because the proton or deuteron in E* is covalently linked to the excited delocalized system of electrons. The reduced intersystem crossing is apparently overcompensating the loss in quantum yield for the formation of E*.

In contrast to the intensity enhancements just mentioned, the deuteration of HMMQ causes a reduction in the intensity of the band F_Z of the solution in *n*-hexane (Figure 12). Apparently, the proton tunneling rate in the primary excited state is then slower than in the case of the solution in 1,4-dioxane and competes less effectively with vibrational relaxation. The reduction in the tunneling rate is to be expected, because the additional H bond of the proton in E* with 1,4-dioxane does not only reduce the dissociation energy of the intramolecular H bond in Z*, but also lowers the barrier for tunneling in E*. The slight decrease in the height of the shoulder on the blue edge of the main band seems to arise from the decreasing contribution of the band F_Z in this region of overlap with the band F_E. A similar reduction in tunneling barrier, caused by additional H bonding to a solvent molecule, explains why the Z* form of HMMN does not appear when it is dissolved in *n*-hexane but can be seen clearly in the case of solutions in, for example, 1,4-dioxane.

The rate constant γ_{K1} is thermally activated and shows Arrhenius behavior in the case of HMMQ in *n*-hexane/5% 1,4-dioxane (Table 1). The significant isotope effect of γ_{K1} in Table 2 suggests that γ_{K1} does not exhibit Arrhenius behavior in the case of HMMQ in neat 1,4-dioxane because it is unlikely that the rotational Brownian motion of the side group (k_r) is affected by the isotopic substitution. Equation 44 should apply in that case; that is, $\gamma_{K1} = (k_X + k_r)$. The isotope effect in γ_{K1} can then be attributed to an enhancement of k_X caused by the substitution. This is not unreasonable, because an intramolecular H bond still exists in X*. Similar increases in decay constants, arising from the isotopic substitution, are found in the case of the fluorescence decay of 7-HQ in 1,4-dioxane and in the case of the decay of the band F_E of HMMN in 1,4-dioxane (Table 2). Hydrogen bonding of 1,4-dioxane to the excited solute is involved in all these three cases. The solution of HMMN in neat *n*-hexane exhibits a decrease in the decay constant of the band F_E with isotopic substitution in contrast to the three previous cases, but as to be expected when the decay is dominated by intersystem crossing from the vibrationless substate. However, this is no longer the case when the solvent is 1,4-dioxane. The conclusion that, in the case of HMMN, excited vibrational substates of E* are thermally populated and the observed T dependence of the rate constants γ_Z, γ_{K1}, and γ_{K2} of HMMQ lead to the suggestion that the radiationless decay (other than chemical conversion) proceeds through a doorway state reached by thermal excitation of a low frequency vibration whose frequency is sensitive to the deuterium substitution in the case of the X* state of HMMQ, of the E* state of HMMN, and of the fluorescent state of 7-HQ in neat 1,4-dioxane. Then, the increase in rate constant caused by deuteration can be explained simply as the direct consequence of the increased thermal population of the doorway state.

The combined intensity of the bands F_E and F_Z of HMMN in 1,4-dioxane decays single exponentially (Table 2). This result means that the states E* and Z* are being interconverted much faster than they decay. Despite the increase in the decay constant on deuteration, a gain in fluorescence from E* is seen in Figure 10 to result from the deuteration. The explanation for this resalt is that the proton tunneling rate for the formation of Z* gets smaller and leads to a larger relative population of the E* state.

Conclusions

The requirement of polar solvents to achieve long-distance photoinduced intramolecular proton transfer in HMMQ in liquid solutions does not arise from the need for bulk solvent electric polarization to stabilize polar or charged intermediates, but is a consequence of the need to lower the dissociation energy of the intermolecular H bond in the excited molecule by additional H bonding of the proton to a solvent molecule. The proton in the OH group may participate simultaneously in an intramolecular and an intermolecular H bond when HMMQ is dissolved in solvents containing proton-accepting molecules. A ground-state equilibrium is established between the bare form of the solute and the solute−solvent complex involving the additional H bond with the solvent molecule. Optical excitation of the bare form does not lead to formation of the excited keto form K*, despite the formation of the excited zwitterionic form Z*. The proton transfer in the primary excited bare form of HMMQ proceeds by tunneling and is completed prior to relaxation of the excess energy deposited with the excitation. Upon vibrational relaxation, the excited bare form E* can no longer be converted into Z*. The intramolecular H bond in the bare form of Z* is too strong to be broken thermally at ~300 K. The dissociation

energy of this bond is lowered by an additional (intermolecular) H bond and as a consequence the available excess excitation energy after excitation is then sufficient to break the intermolecular H bond. The protonated side group in Z* can then start its rotational Brownian motion to deliver the proton at the N atom in the quinoline ring, as required for the formation of K*. After the bare form of Z* is generated from bare E*, a complex {Z*S} is formed involving an additional H bond of Z* with a proton-accepting solvent molecule S. The observed fluorescence band F_Z of HMMQ in, for example, *n*-hexane/5%1,4-dioxane, arises predominantly from emission by {Z*S}. The species E* and {Z*S} do not get interconverted and neither is there reverse conversion of {Z*S} into Z*. The scheme for the conversion of the excited species generated by excitation of HMMQ accounts adequately for the observed *T* dependence of the intensities of the bands and the appearance of isoemissive points in the fluorescence spectrum when either *T* or C_S is varied and also for the kinetic features. The decay of the band F_Z is dominated (at ~300 K) by radiationless decay through an excited state of a low-frequency vibration that is sensitive to deuteration of the OH group in HMMQ. The enhancement of the intensity of the band F_Z of HMMQ in 1,4-dioxane caused by deuteration can be attributed to a reduction in the rate of vibrational relaxation of the primary excited enol form, which favors conversion into Z* over formation of the vibrationless state of E*. The blue shift of the main fluorescence band of HMMN in *n*-hexane on deuteration arises from contributions of thermally populated excited states of low-frequency vibrations involving motion of the proton (deuteron) to the emission.

References and Notes

(1) Kemp, D. S. *Nature* **1995**, *373*, 196.

(2) Gutman, M.; Nachliel, E. *Annu. Rev. Phys. Chem.* **1997**, *48*, 329.

(3) Cukier, R. I.; Nocera, D. G. *Annu. Rev. Phys. Chem.* **1998**, *49*, 337.

(4) Konijnenberg, J.; Huizer, A. H.; Chaudron, F. Th.; Varma, C. A. G. O.; Marciniak, B.; Paszyc. S. *J. Chem. Soc., Faraday Trans. 2* **1987**, *83*, 1475.

(5) Konijnenberg, J.; Huizer, A. H.; Varma, C. A. G. O. *J. Chem. Soc., Faraday Trans. 2* **1988**, *84*, 1163.

(6) Konijnenberg, J.; Ekelmans, G. B.; Huizer, A. H.; Varma, C. A. G. O. *J. Chem. Soc., Faraday Trans. 2* **1989**, *85*, 39.

(7) Konijnenberg, J.; Huizer, A. H.; Varma, C. A. G. O. *J. Chem. Soc., Faraday Trans. 2* **1988**, *84*, 363.

(8) Barbara, P. F. In *Tunneling*; Jortner, J., Pullman, B., Eds.; Reidel: Dordrecht, 1986; p 139.

(9) Konijnenberg, J.; Huizer, A. H.; Varma, C. A. G. O. *J. Chem. Soc., Faraday Trans. 2* **1989**, *85*, 1539.

(10) Thistlewaite, P. J.; Corkill, P. J. *Chem. Phys. Lett.* **1982**, *85*, 513.

(11) Thistlewaite, P. J. *Chem. Phys. Lett.* **1983**, *96*, 509.

(12) Schwartz, B. J.; Peteanu, L. A.; Harris, C. B. *J. Phys. Chem.* **1992**, *96*, 3591.

(13) Jalink, C. J.; Van Ingen, W. M.; Huizer, A. H.; Varma, C. A. G. O. *J. Chem. Soc., Faraday Trans.* **1991**, *87*, 1103.

(14) Jalink, C. J.; Huizer, A. H.; Varma, C. A. G. O. *J. Chem. Soc., Faraday Trans.* **1992**, *88*, 1643.

(15) Jalink, C. J.; Huizer, A. H.; Varma, C. A. G. O. *J. Chem. Soc., Faraday Trans.* **1992**, *88*, 2655.

(16) Jalink, C. J.; Huizer, A. H.; Varma, C. A. G. O. *J. Chem. Soc., Faraday Trans.* **1993**, *89*, 1677.

(17) Geerlings, J. D.; Huizer, A. H.; Varma, C. A. G. O. *J. Chem. Soc., Faraday Trans.* **1997**, *93*, 237.

(18) Geerlings, J. D.; Varma, C. A. G. O. *J. Photochem. Photobiol. A* **1999**, *129*, 129.

(19) Köhler, G.; Wolschann, P. *J. Chem. Soc., Faraday Trans. 2* **1987**, *83*, 513.

(20) Geerlings, J. D.; Varma, C. A. G. O.; van Hemert, M. C. *J. Phys. Chem. B* **2000**, *104*, 56.